International Journal on Advanced Science Engineering Information Technology

Vol.14 (2024) No. 2
ISSN: 2088-5334

Electrical Properties for Non-destructive Determination of Free Fatty Acid and Moisture Content in Oil Palm Fruit

Verra Mellyana [a,b], I Wayan Budiastra [a,c,*], Irmansyah [d], Yohanes Aris Purwanto [a]

[a] *Department of Mechanical and Biosystem Engineering, IPB University, Bogor, Indonesia*
[b] *Agency of Agricultural Extension and Human Resources Development (IAAEHRD), Ministry of Agriculture, Indonesia*
[c] *Center for Research on Engineering Application in Tropical Agriculture, IPB University, Bogor, Indonesia*
[d] *Department of Physics, IPB University, Bogor, Indonesia*
*Corresponding author: *wbudiastra@apps.ipb.ac.id*

***Abstract*—FFA content is one of the essential qualities of oil palm fruit. FFA content exceeding 5% is considered unsuitable for human consumption. Commonly, FFA content is determined by chemical methods in the laboratory, but it is destructive, time-consuming, and costly. Several non-destructive methods have been investigated, but a maturity prediction approach has been primarily used with no direct relation to FFA content. Thus, there is a pressing need for a non-destructive framework to assess the FFA levels in the oil palm fruit directly. An attempt has been explored using a non-destructive palm fruit quality assessment that relied on electrical properties (impedance, admittance, resistance, and capacitance) in the frequency range from 50 Hz to 5 MHz was investigated to predict FFA and moisture content directly. Two statistical analyses were employed: stepwise multiple linear regressions (MLR) and artificial neural networks (ANN) to calibrate and validate electrical properties with FFA and moisture content. The best-performing models ANN showcased significant results: r= 0.96, R^2=0.92, SEC at 0.86%, SEP at 0.97%, CV at 19.45%, consistency at 88.54, and RPD at 3.43 for FFA prediction, and r= 0.99, R^2=0.98, SEC at 3.09 %, SEP at 3.46 %, CV at 5.44 %, consistency at 89.08 and RPD at 7.02 for predicting moisture content. In modeling oil palm quality determination, applying the ANN method significantly improved model performances, demonstrating its efficacy in predicting non-destructively both FFA levels based on admittance and moisture content based on impedance.**

***Keywords*— Artificial neural network; electrical properties; free fatty acid; moisture content; oil palm fruit.**

Manuscript received 4 Jan. 2024; revised 29 Mar. 2024; accepted 16 Apr. 2024. Date of publication 30 Apr. 2024.

I. INTRODUCTION

The increasing demand for vegetable oil poses a challenge in agricultural management [1], especially concerning the rapid acidification of oil due to heightened lipase activity. This process primarily releases free fatty acids (FFA) from the mature and bruised mesocarp of the oil palm fruit. Elevated acidity significantly compromises the oil quality, as FFA content exceeding 5% is considered unsuitable for human consumption. This accelerated acidification poses challenges for smaller farming entities without proper milling infrastructure, leading to the rejection of overly ripe fruit by processing mills. Delayed harvesting of oil palm fruit results in an increased FFA content in the oil, with studies indicating potential FFA levels could exceed 12% when fruit is left unharvested for an extended post-ripening period [2], [3]. The maturity of fresh oil palm fruit is a crucial factor in determining the quality of the resulting oil [4]. Harvest timing significantly influences the FFA content, particularly the palmitic FFA within the produced oil palm fruit. Overripe fruit yields high FFA content in the oil, while unripe fruit contains low FFA and results in lower oil extraction [5],[6]. The maturity level of oil palm fruit is a determining factor [7] in producing superior-quality oil with low FFA content.

Elevated FFA levels indicate oil deterioration, which can directly impact the market price of the oil. FFA can alter the oil's flavor, resulting in an undesirable taste, and may contain potentially hazardous oxidized compounds. The raw palm oil industry plays a vital role in producing high-purity and stable palm oil before it is sent to the palm oil processing facility. Therefore, adhering to regulatory standards is crucial to keep FFA levels below the set threshold of 5% [8].

The conventional method for determining the fatty acid content in oil palm fruit uses a chemical approach, which is complicated, time-consuming, and destructive. Thus, there is

a pressing need for a non-destructive framework to assess the FFA levels in the fruit directly and determine moisture content based on its electrical characteristics. It offers accuracy, rapidity, cost-effectiveness, and eco-friendliness.

Currently, research using electrical characteristics is frequently conducted to determine the maturity level of various fruits, such as apples, lettuce, mangoes, strawberries, citrus from Garut [9], [10], lemons, tomatoes [11], bananas [12] and other food items, including spinach leaf powder [13], milk [14], meat [15], a lamb [16], yogurts [17], honey [18] and oil palm fruit [7], [19]. Recent advancements have shown that sensors using electrical properties are instrumental in determining oil and water content in oil palm fruit [19]. The non-destructive methods for determining the FFA content of oil palm fruit directly based on electrical properties have yet to be conducted.

Applying electrical characteristics to assess FFA levels in oil palm fruit is essential to evaluate oil content accurately and efficiently, ultimately leading to improved quality and profitability for palm oil businesses. In this study, measurements will be conducted on fruitlets as an initial step to explore the potential of electrical properties for determining FFA levels in these fruitlets. This study aims to develop calibration models to enhance the precision of measuring FFA and moisture content in oil palm fruit.

II. Materials and Method

A. Initial Phase of the Research

1) Oil palm fruit: The oil palm fruit belonging to the 106 Tenera variety was obtained from the Cikabayan plantation at Bogor Agricultural University in Bogor, Indonesia. These fruits were meticulously categorized based on their respective stages of maturation, forming distinct groups. The groups consisted of 12 samples from the 3-month (3M), 12 samples from 4-month (4M), 12 samples from 4-month and 1-week (4M1W), nine samples from 4-month and 2-weeks (4M2W), nine samples from 4-month and 3-weeks (4M3W), nine samples from 5-month (5M), nine samples from 5-month and 1-week (5M1W), 12 samples from 5-month and 2-weeks (5M2W), 12 samples from 5-month and 3-weeks (5M3W), and ten samples from 6-month (6M) stages. Following initial procedures encompassing cleaning, precise weighing, and measurement of physical dimensions, the study further included essential electrical and chemical measurements as integral facets of the research.

2) Electrical properties measurements: The evaluation of oil palm fruit in terms of electrical properties characteristics was performed using a 30 mm long and 20 mm wide copper ellipse. This specific copper ellipse was connected to an LCR Hitester 3532-50 (Hioki, Tokyo, Japan) and assessed across 200 data points ranging from 50 Hz to 5 MHz. Before conducting the measurements, the LCR meter underwent calibration according to the manufacturer's prescribed procedure to minimize potential systematic errors. All evaluations were carried out under room temperature conditions. The oil palm fruit was individually measured once, divided by their respective weights, and positioned between two copper plates connected to the LCR meter. The measured electrical properties include impedance [11], [19], [20], [21], [22], [23], [24], [25], admittance, resistance, and capacitance[26].

3) FFA and moisture content measurements: The acid value is the number of milligrams of NaOH to neutralize the FFA in one gram of oil or fat. A higher acid value indicates more FFA, potentially originating from oil hydrolysis or insufficient processing. The higher the acid value, the lower the quality. FFA (Eq. (1) is calculated based on AOAC 940.28.2005[27].

$$FFA \text{ (as oleate, \% by weight)} = T\ x\ 0.05\ x\ 1.99 \quad (1)$$

where T is the titrant volume of 0.1 M NaOH (ml)

The moisture content extraction followed the AOAC Official Method 930.04 [27], utilizing aluminum cups, a desiccator, an oven, and an analytical balance within the oven set at a temperature of 101±1 ºC. The moisture content of each fruit was computed using (Eq. (2).

$$\text{Moisture Content (\%)} = \left(\frac{W-W_1}{W}\right) x100 \quad (2)$$

where W_1 is residue weight (grams) and W is Sample weight for testing (grams).

B. Implementation Stage of the Research

Electrical property spectra data, such as impedance, admittance, resistance, and admittance, were processed using MLR calibrated with FFA or moisture content. From the MLR calibration results, the most influential frequency was identified. This significant frequency data was then utilized as input for the ANN in prediction and calibration processes. The main objective is to achieve a regression model with optimal performance and minimal error (Fig.1).

1) Multiple linear regression (MLR): The widely used multiple linear regression (MLR) analysis technique [28], [29] is crucial in fine-tuning spectral analysis models within the visible-near-infrared light spectrum. However, in this specific study, the available sample size was insufficient compared to the variables in the electrical spectral dataset, making it unfeasible to establish the MLR model due to collinearity issues directly. Researchers employed a stepwise method to overcome this limitation and improve accuracy and efficiency. This approach effectively reduced variable collinearity, leading to a notable enhancement in predictive accuracy while using fewer variables than the conventional MLR model. The development of the Stepwise MLR model was facilitated by IBM's statistical engineering software in the United States. The resulting MLR prediction models were structured based on multiple segments of reflectance frequency. Although assessing the significance of each frequency segment is challenging due to collinearity concerns, the model's interpretation remains viable. The FFA and moisture content prediction was conducted using Unscramble 10 software by CAMO.

The formulation representing the FFA estimation model was delineated as Eq. (3):

$$FFA\ (\%) = \beta + \beta_1 f_1 + \beta_2 f_2 + \beta_3 f_3 + \cdots + \beta_n f_n \quad (3)$$

where FFA % was the FFA prediction value, β was constant, β_n was coefficient of nth predictor, and f_n was the pre-treated spectra value of the nth predictor at specific frequencies. The

formulation representing the moisture content estimation model could be articulated in Eq. (4):

$$MC\ (\%) = a + a_1 f_1 + a_2 f_2 + a_3 f_3 + \cdots + a_n f_n \quad (4)$$

where MC % was moisture content prediction value, α was constant, α_n was coefficient of nth predictor, and f_n was the pre-treated spectra value of the nth predictor at specific frequencies.

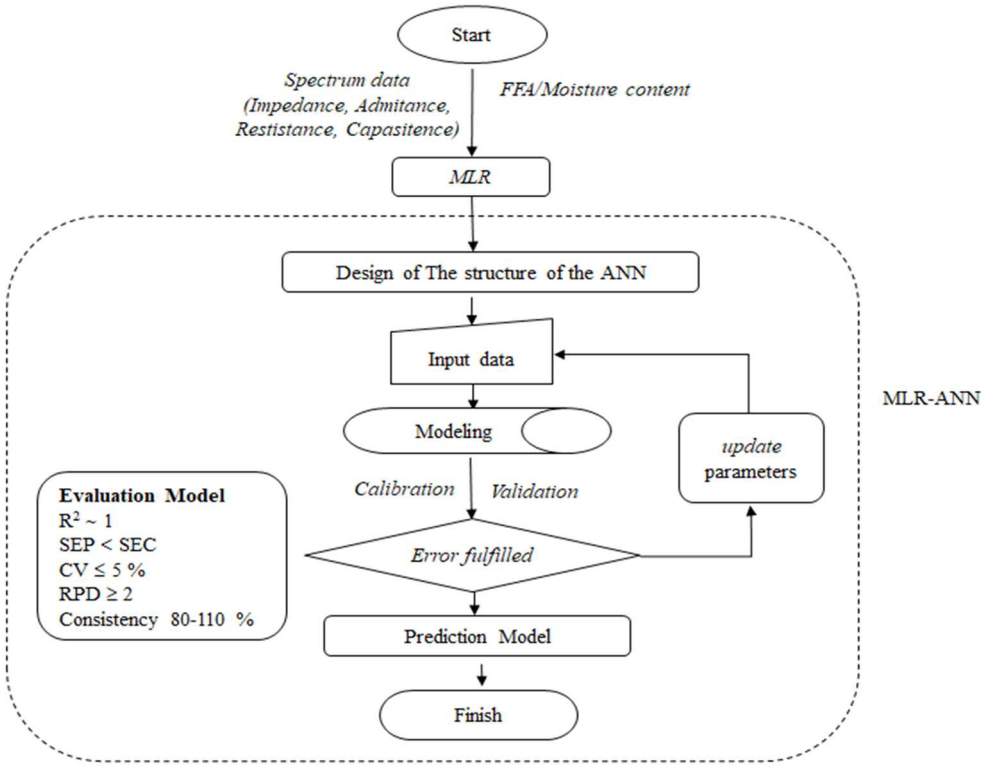

Fig. 1 Data processing flowchart.

2) Artificial neural network (ANN): The Artificial Neural Network (ANN) replicates the neural network of the human brain, consisting of interconnected neurons that process information across layers. Each neuron receives input, performs computations, and generates output via activation functions. ANN encompasses input, hidden, and output layers [28], [30], which are responsible for data reception, computation, and outcome generation. By adjusting neuron connections (known as "weights"), it learns from training data to refine its performance. Renowned for its application in pattern recognition, prediction, language processing, and more, ANN excels in handling intricate tasks and learning from diverse datasets, proving vital in numerous applications.

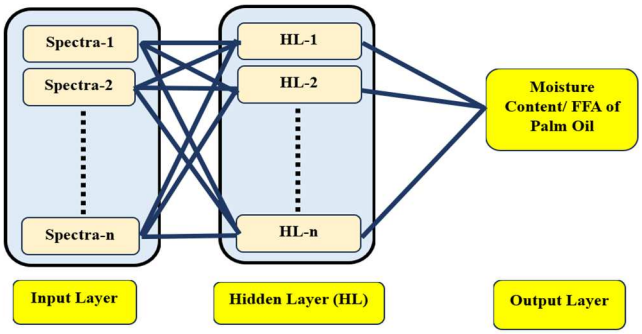

Fig.2 The network diagram of ANN

ANN was a hybrid approach combining MLR with artificial neural networks. In this study, multilayer neural network models were developed using acquired electrical spectra as input predictor variables. The network diagram of the ANN can be seen in Fig.2. These models, featuring hidden layers, were created through RapidMiner software [31], [32] for data analysis. They were utilized to estimate various oil palm qualities, including FFA and moisture content measurements. The process encompassed training a sequence of multilayer neural-net models comprising hidden and output layers. This study employed the spectrum of electrical properties obtained from selecting the best frequencies using the MLR method as input in an ANN. This was done to predict the FFA and moisture content.

C. Evaluation

The model performance was evaluated by comparing the calibration and validation. Approximately two-thirds of the samples were employed for calibration, while the remaining one-third was set aside for validation, enabling the creation of calibration and validation datasets. The evaluation of the FFA and moisture content prediction of the calibration model will involve a thorough analysis utilizing essential statistical metrics such as the coefficient of determination (R^2) (Eq. (5)), the correlation coefficient (r) (Eq. (6)), standard error calibration (SEC) (Eq. (7)), standard error prediction (SEP) (Eq. (8)), coefficient of variance (CV) (Eq. (9)), consistency (Eq. (10)) and ratio of standard deviation (RPD) (Eq. (11)). These metrics play a crucial role in assessing the precision and accuracy of the calibration model, ensuring dependable measurements of FFA and moisture content. A model is

considered good if $R^2 \sim 1$, SEP < SEC, CV ≤ 5 %, RPD ≥ 2, and consistency 80-110 % [33].

$$R^2 = \frac{\sum_1^n[(Y_{ref}-\overline{Y_{ref}})][(Y_{spectra}-\overline{Y_{spectra}})}{\sum_1^n(Y_{ref}-\overline{Y_{ref}})^2 \sum_1^n(Y_{spectra}-\overline{Y_{spectra}})^2} \quad (5)$$

$$r = \sqrt{R^2} \quad (6)$$

$$SEC = \sqrt{\frac{\sum_1^n(Y_{ref}-Y_{spectra})^2}{n}} \quad (7)$$

$$SEP = \sqrt{\frac{\sum_1^n(Y_{ref}-Y_{spectra}-bias)^2}{n-1}};\ bias = \frac{\sum_1^n(Y_{ref}-Y_{spectra})}{n} \quad (8)$$

$$CV = \frac{\sum_1^n(Y_{ref}-\overline{Y_{ref}})^2}{\overline{Y_{ref}}} x100\%\ or\ CV = \frac{SD}{mean} x100\% \quad (9)$$

$$Consistensi = \frac{SEC}{SEP} x100\%; \quad (10)$$

$$RPD = \frac{SD}{SEC} \quad (11)$$

III. Results and Discussion

A. Electrical Characteristics

1) Impedance characteristics of oil palm fruit: Impedance on a capacitor plate acts as resistance against the applied electric field. Oil palm fruit, with its water (resistive) and oil (capacitive) components, creates impedance by combining resistance and capacitance, forming the total resistance impedance (Z). The magnitude of electrical impedance depends on resistance, frequency, and reactance. Lower frequencies emphasize significant reactance, leading to higher impedance, while higher frequencies reduce reactance, resulting in lower impedance. Impedance represents total resistance under alternating current.

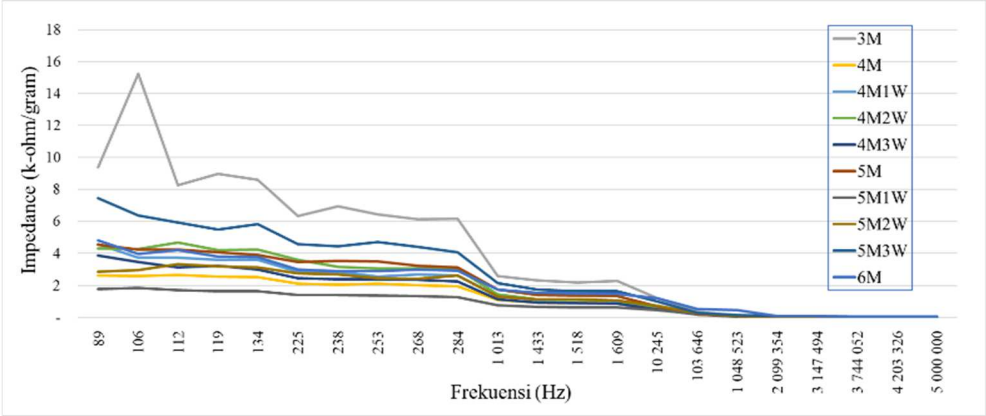

Fig. 3 The spectrum of impedance per unit weight across diverse maturity levels.

As frequency increases, both resistance and reactance decrease, lowering impedance. Resistance and reactance collaborate to determine impedance, which decreases with increasing frequency. Decreasing impedance due to increased frequency also occurs in citrus fruits. Fig.3 illustrates an increase in impedance beyond 89 Hz, followed by a decline at frequencies surpassing 1 MHz. At lower frequencies, high impedance values imply current flow restricted to the extracellular region. Conversely, lower impedance at higher frequencies facilitates current passage within the cells.

2) Admittance characteristics of oil palm fruit: Admittance, the reciprocal of impedance, gauges a circuit's capability to carry alternating current at a particular frequency. It comprises two constituents: conductance admittance, which represents the conductive aspect, and susceptance admittance, signifying the reactive element. In Fig.4, the admittance of oil palm fruit exhibited an upward trend at frequencies exceeding 1 MHz. It persisted up to 5 MHz, illustrating distinctions among different maturity stages of oil palm fruit.

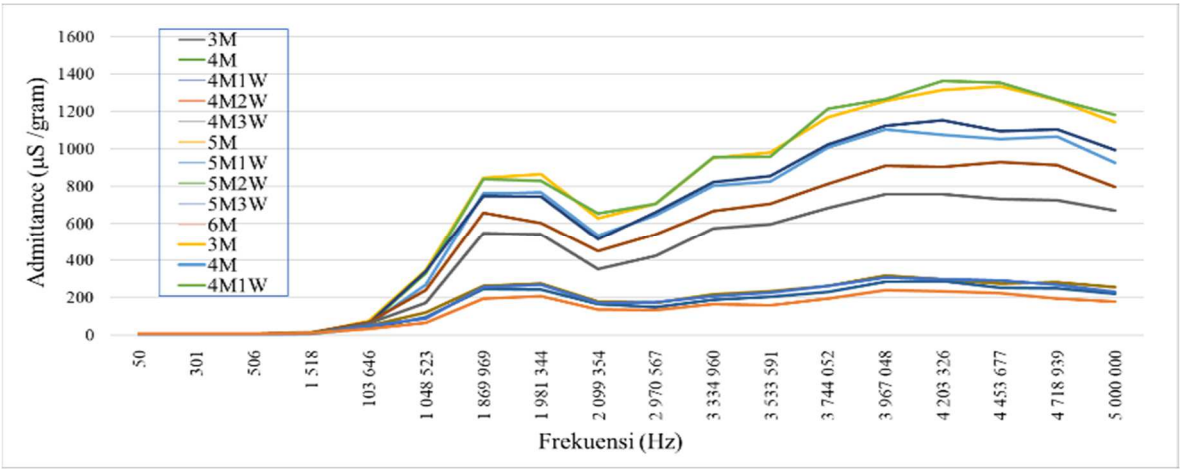

Fig. 4 The spectrum of admittance per unit weight across diverse maturity levels.

3) Resistance characteristics of oil palm fruit: Resistance characterizes an object's capacity to hinder the passage of electrical current. The presence of oil content within a liquid can impact its resistance due to the influence of dissolved oil on the liquid's chemical properties. The incredible water content in a liquid enhances its electrical conductivity. This phenomenon was apparent in Fig.5, where oil palm fruit at three months of maturity demonstrated elevated resistance, impeding electrical current flow. Conversely, fruit aged four months displayed diminished resistance, facilitating electrical current flow. As maturity progressed, resistance declined, reducing impedance to the electrical current flow. Fig.5 illustrates an increase in resistance beyond 71 Hz, followed by a high decline at frequencies surpassing 10 kHz.

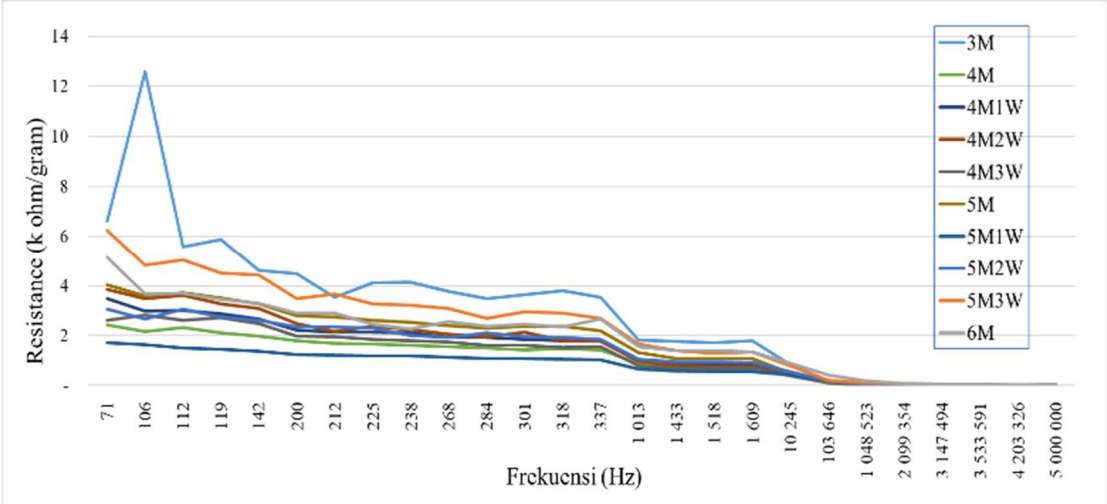

Fig. 5 The spectrum of resistance per unit weight across diverse maturity levels.

4) Capacitance characteristics of oil palm fruit: Capacitance defines a capacitor's capacity to hold energy and electric charge. Including a dielectric substance in the capacitor led to an augmentation in capacitance. In Fig.6, the capacitance of oil palm fruit across different maturity stages exhibited variations at frequencies surpassing 50Hz, followed by a decline at frequencies exceeding 1 kHz to 5 MHz.

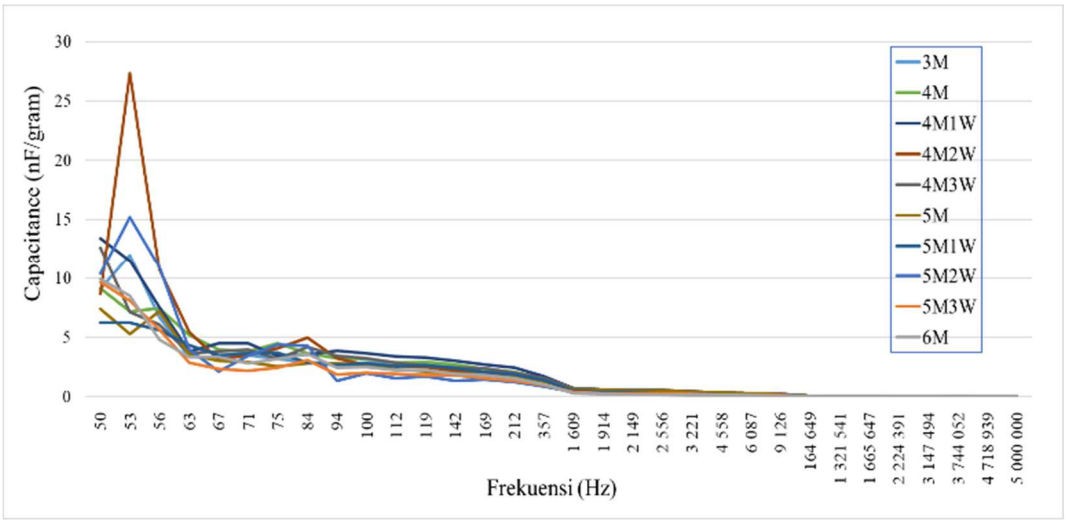

Fig. 6 The spectrum of capacitance per unit weight across diverse maturity levels.

B. Chemical Properties of Oil Palm Fruit

Descriptive statistics presented in Table 1 outline the FFA and moisture content levels. The data illustrates considerable variability within Tenera oil palm samples, with FFA levels ranging from 0% to 14.87% and moisture content ranging from 27.75% to 86.39%. The FFA in oil palm fruit varies throughout its maturity stages. Specifically, the average FFA content is 0.00% at three months of maturity. Subsequently, at four months, it increases to an average of 5.39%, followed by 5.85% at four months and one week, 6.28% at four months and two weeks, 6.01% at four months and three weeks, 3.76% at five months, 4.02% at five months and one week, 4.53% at five months and two weeks, 4.22% at five months and three weeks, and finally stabilize at an average of 4.14% by six months of maturity.

The moisture content within oil palm fruit is notably affected by its maturity level, decreasing progressively during ripening. Specifically, at three months of maturity, the average moisture content is 85.32%. Subsequently, at four

months, it reduces to an average of 82.11%, followed by 79.47% at four months and one week, 74.47% at four months and two weeks, 61.49% at four months and three weeks, 57.22% at five months, 34.39% at five months and one week, 38.63% at five months and two weeks, 34.77% at five months and three weeks, and finally, reaches an average of 34.10% at six months of maturity.

TABLE I
STATISTICAL REFERENCE DATA OF TENERA OIL PALM

Chemical properties	stages of maturation	Average (%)	Deviation standard (%)	Minimum (%)	Maximum (%)
FFA	3M	0	0	0	0
	4M	5.39	3.30	2.32	11.75
	4M1W	5.85	6.35	0	14.87
	4M2W	6.28	2.83	3.94	11.87
	4M3W	6.01	0.76	5.15	7.14
	5M	3.76	1.47	0.28	5.28
	5M1W	4.02	0.48	3.56	5.19
	5M2W	4.53	0.56	3.63	5.27
	5M3W	4.22	1.33	1.80	5.93
	6M	4.14	0.41	3.27	4.54
Moisture content	3M	85.32	0.87	83.85	86.39
	4M	82.11	3.05	77.84	85.24
	4M1W	79.47	5.30	71.96	84.91
	4M2W	74.47	6.45	63.39	82.32
	4M3W	61.49	14.35	40.79	78.75
	5M	57.22	11.62	45.75	72.80
	5M1W	34.39	3.60	29.76	40.21
	5M2W	38.63	4.33	28.82	44.52
	5M3W	34.77	4.49	30.90	48.24
	6M	34.10	7.17	27.75	53.15

C. MLR Calibration and Prediction for FFA and Moisture Content

Determining FFA and moisture content levels based on electrical properties (impedance, admittance, resistance, and capacitance) was conducted utilizing MLR analysis, as presented in Table 2. The most accurate prediction of FFA was achieved using the electrical property of admittance, demonstrating the highest R^2 value (0.90), highest r (0.95), lowest SEC (0.94), SEP (0.71), and CV (18.21), along with the highest RPD (3.14). These values outperformed predictions made using impedance, resistance, and capacitance (R^2 0.16~0.55, r 0.4~0.74, SEC 1.98~2.70, SEP 1.66~2.89, CV 44.87~61.13 and RPD 1.09~1.49).

Regarding moisture content, the most accurate prediction of moisture content levels was attained using impedance electrical property, which demonstrated the highest R^2 value (0.96), highest r (0.98), lowest SEC (4.78), SEP (4.25), and CV (8.15), alongside the highest RPD (4.68). These values surpassed predictions using admittance, resistance, and capacitance (R^2 0.90~0.91, SEC 6.38~7.21, SEP 4.5~7.09, CV 11.25~12.71 and RPD 3.00~3.39).

TABLE II
CALIBRATION RESULTS FOR FFA AND MOISTURE CONTENT BASED ON IMPEDANCE, ADMITTANCE, RESISTANCE, AND CAPACITANCE.

Electrical properties	R^2	r	SEC (%)	SEP (%)	CV (%)	RPD	Bias	CI
					FFA			
Impedance	0.16	0.40	2.70	2.89	61.13	1.09	0.25	93.35
Admittance	**0.90**	**0.95**	**0.94**	**0.71**	**18.21**	**3.14**	**0.02**	**131.13**
Resistance	0.40	0.63	2.28	2.18	51.71	1.29	0.08	104.36
Capacitance	0.55	0.74	1.98	1.66	44.87	1.49	0.22	119.12
					Moisture Content			
Impedance	**0.96**	**0.98**	**4.78**	**4.25**	**8.15**	**4.68**	**-0.14**	**112.47**
Admittance	0.90	0.95	6.96	5.78	12.27	3.11	-0.33	120.42
Resistance	0.91	0.96	6.38	4.50	11.25	3.39	-0.86	141.95
Capacitance	0.90	0.95	7.21	7.09	12.71	3.00	0.25	101.66

Ci: consistency
Impedance, Resistance (kohm/gram); Admittance(μsiemens/gram)
Capacitance (nfarad/gram)

Overall, the utilization of specific electrical properties for predicting FFA and moisture content levels exhibited distinct performances, with admittance proving superior for FFA level estimation and impedance excelling in moisture content prediction.

1) FFA Prediction based on Admittance: The conventional method for assessing FFA content in oil palm fruit involves a wet-chemical process demanding substantial resources in time, personnel, and glassware for standard

reagent preparation and analysis. Therefore, exploring alternative methods is crucial to address these resource-intensive procedures. In the case of FFA prediction, the models employed the electrical property of admittance, resulting in the highest values of R^2=0.90 and r=0.95 (Table 2), of which 69 datasets were used for calibration and 31 datasets for validation.

The presence of excessive moisture content in oil palm fruit significantly impacts the quality of the extracted oil. Elevated moisture levels in the fruit pose a considerable risk to oil quality, primarily by escalating the likelihood of oxidation and free fatty acid formation. Consequently, these factors can detrimentally influence the sensory attributes such as taste, aroma, and stability of oil palm fruit. To estimate FFA, a predictive model utilized admittance spectral data obtained immediately after harvesting oil palm fruit.

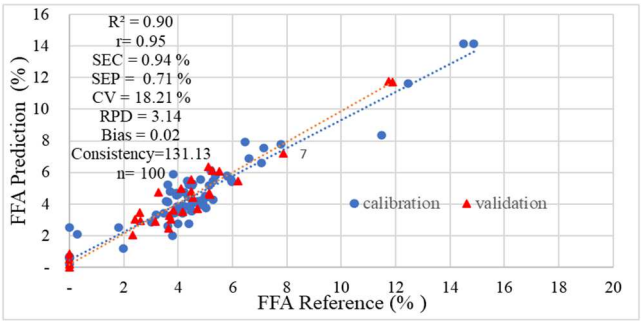

Fig. 7 Calibration and validation results for the FFA model of the oil palm fruit using the MLR method

The development of this predictive model necessitated meticulous consideration of 28 predictor variables. The predictors used in the FFA model were pre-treated admittance data at frequency of 67, 94, 100, 126, 159, 3040, 13682, 14497, 21735, 24401, 25855, 36584, 65245, 207520, 219880, 261555, 392141, 415497, 440244, 523685, 587925, 785145, 1048523, 1247254, 1400252, 1764854, 2356877, dan 3334960 Hz.

The variables integrated into the model suggest that significant variations in oil palm fruit, FFA, could be identified by analyzing the admittance at this specific frequency. Both the calibration and validation stages demonstrated adequate performance for the FFA prediction model, as depicted in Fig.7. During the calibration process, the model displayed an R^2 value of 0.90, a correlation coefficient (r) of 0.95, SEC at 0.94%, SEP at 0.71%, CV at 18.21%, Consistency of 131.13, and an RPD of 3.14. These parameters collectively indicate a high level of accuracy in predicting moisture content. An RPD value surpassing 2.5 suggested that this model was excellent classified [33].

2) Moisture content calibration and prediction based on impedance: For moisture content, the models utilized the electrical property of impedance, resulting in the highest values of R^2=0.96 and r=0.98 (Table 2), which 74 datasets were used for calibration and 32 datasets for validation.

In the development of this model, the inclusion of predictors was carefully considered, amounting to a total of 21, along with the incorporation of a constant value. The predictors used in the moisture content model were pre-treated impedance data at frequency of 59, 284, 425, 1276, 1914, 2276, 2556, 14497, 61578, 116360, 174455, 261555, 329659, 741010, 1572018, 1981344, 2099354, 2224391, 2970567, 4453677, dan 5000000 Hz. Both the calibration and validation phases demonstrated satisfactory performance for the moisture content prediction model (Fig.8).

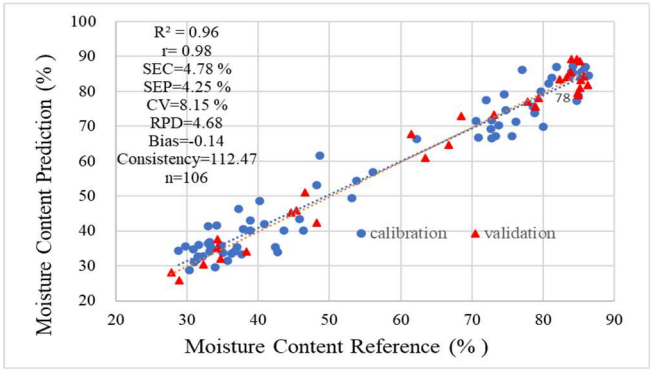

Fig. 8 Plot of reference versus predicted moisture content calibration using MLR method

During calibration, the model exhibited an R^2 of 0.96, a coefficient of correlation (r) of 0.98, SEC at 4.78%, SEP at 4.25%, CV at 8.15%, Consistency of 112.47, and an RPD of 4.68. These metrics collectively denote a high level of precision in forecasting moisture content. An RPD value surpassing 2.5 indicated that this model was excellent classified [33].

D. ANN Calibration and Prediction for FFA and Moisture Content

1) FFA calibration and prediction based on admittance: The ANN models integrated 28 specifically chosen admittance spectra variables acquired through the MLR method. The dataset comprised admittance values at distinct frequencies: 567, 94, 100, 126, 159, 3040, 13682, 14497, 21735, 24401, 25855, 36584, 65245, 207520, 219880, 261555, 392141, 415497, 440244, 523685, 587925, 785145, 1048523, 1247254, 1400252, 1764854, 2356877, and 3334960 Hz, serving as input variables for the ANN.

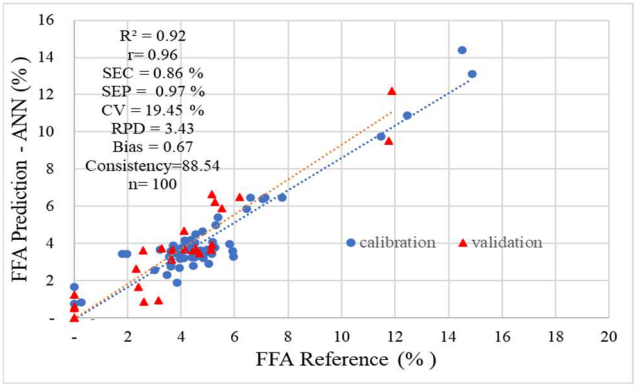

Fig. 9 Plot of reference versus predicted FFA calibration using ANN method.

The best prediction of FFA was achieved by employing an ANN configuration with two hidden layers, featuring 28 nodes representing admittance spectra on the input layer, undergoing 370 training cycles, utilizing a learning rate of 0.019, and employing a momentum value of 0.97. During calibration, the ANN model exhibited an R^2 of 0.92, a coefficient of correlation (r) of 0.96, SEC at 0.86%, SEP at

0.97%, CV at 19.45%, Consistency of 88.54, and an RPD of 3.43 (Fig.9). These metrics collectively denote a high level of precision in forecasting moisture content. An RPD value surpassing 2.5 indicated that this model was excellent classified [33]. The ANN model demonstrates superior performance for FFA compared to the MLR method.

2) Moisture content calibration and prediction based on impedance: The ANN models utilized 21 impedance spectra variables selected through the MLR method. The provided dataset comprises impedance values across a range of frequencies: 59, 284, 425, 1276, 1914, 2276, 2556, 14497, 61578, 116360, 174455, 261555, 329659, 741010, 1572018, 1981344, 2099354, 2224391, 2970567, 4453677, and 5000000 Hz. These values were employed as input variables for the ANN.

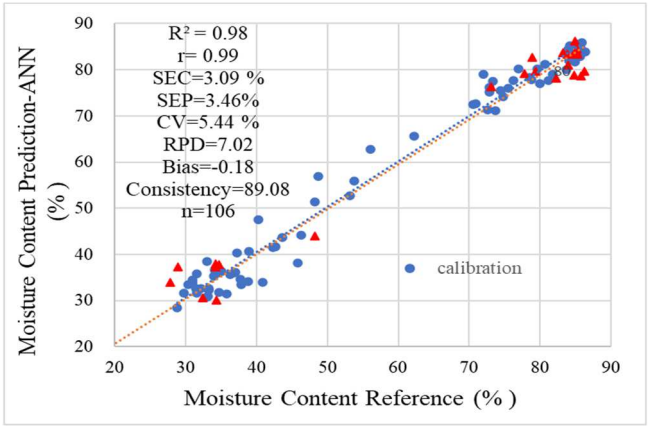

Fig. 10 The plot of reference versus predicted moisture content calibration using the ANN method.

The best prediction of moisture content was achieved by employing an ANN configuration with one hidden layer, featuring 21 nodes representing impedance spectra on the input layer, undergoing 2300 training cycles, utilizing a learning rate of 0.01, and employing a momentum value of 0.91. During calibration, the ANN model exhibited an R^2 of 0.98, a coefficient of correlation (r) of 0.99, SEC at 3.09%, SEP at 3.46%, CV at 5.44%, Consistency of 89.08, and an RPD of 7.02 (Fig.10). An RPD value surpassing 2.5 indicated that this model was excellent classified [33]. The moisture content ANN model demonstrated superior performance compared to the MLR method.

IV. Conclusion

In this study, an admittance was utilized to predict the FFA, while an impedance spectrum was employed to directly predict oil palm's moisture content. Subsequently, these datasets were compared with the outcomes of chemical analysis to develop predictive models. Two methods were used for creating models: MLR and ANN.

The FFA prediction with MLR model involved 28 predictors (admittance spectra), exhibited calibration performance, with an r of 0.95, an R^2 of 0.90, SEC of 0.94%, SEP of 0.71%, CV of 18.21%, Consistency of 131.13, and an RPD of 3.14. Meanwhile, the moisture content prediction-MLR model, comprising 21 predictors (impedance spectra), exhibited calibration performance, with an r of 0.98, an R^2 of 0.96, SEC of 4.78%, SEP of 4.25%, CV of 8.15%, Consistency of 112.47, and an RPD of 4.68.

The FFA prediction by ANN model showcased superior performance compared to the MLR method. This was evidenced by an r of 0.96, an R^2 of 0.92, SEC of 0.86%, SEP of 0.97%, CV of 19.45%, Consistency of 88.54, and an RPD of 3.43. Meanwhile, the moisture content prediction model using ANN demonstrated similarly robust calibration performance, boasting an r of 0.99, an R^2 of 0.98, SEC of 3.09%, SEP of 3.46%, CV of 5.44%, Consistency of 89.08, and an RPD of 7.02. Overall, the models generated through ANN methods exhibited superior performance compared to those developed using the MLR Method.

The following research will determine the oil and FFA content of FFB (Fresh Fruit Bunches) directly based on its electrical properties. FFB refers to the bunches of oil palm fruit harvested before processing. These fresh fruit bunches are the primary raw material from which palm oil is extracted.

Acknowledgment

The authors are grateful to the Agency of Agricultural Extension and Human Resources Development (IAAEHRD), Ministry of Agriculture, Indonesia, as well as the Directorate General of Higher Education, Research, and Technology (DGHERT) under the Ministry of Education, Culture, Research, and Technology (MOECRT) of the Republic of Indonesia for the Research Grant of Program Implementation Contract for the Year 2023: 102/E5/PG.02.00.PL/2023.

References

[1] X. J. Tan, W. L. Cheor, K. S. Yeo, and W. Z. Leow, "Expert systems in oil palm precision agriculture: A decade systematic review," *Journal of King Saud University - Computer and Information Sciences*, vol. 34, no. 4, pp. 1569–1594, Apr. 2022, doi:10.1016/j.jksuci.2022.02.006.

[2] A. R. M. Akbar, A. D. Wibowo, and R. Santoso, "Investigation on the Optimal Harvesting Time of Oil Palm Fruit," *Jurnal Teknik Pertanian Lampung (Journal of Agricultural Engineering)*, vol. 12, no. 2, p. 524, Jun. 2023, doi: 10.23960/jtep-l.v12i2.524-532.

[3] E. Edyson, F. Murgianto, A. Ardiyanto, E. J. Astuti, and M. P. Ahmad, "Preprocessing Factors Affected Free Fatty Acid Content in Crude Palm Oil Quality," *Jurnal Ilmu Pertanian Indonesia*, vol. 27, no. 2, pp. 177–181, Apr. 2022, doi: 10.18343/jipi.27.2.177.

[4] E. Salim and Suharjito, "Hyperparameter optimization of YOLOv4 tiny for palm oil fresh fruit bunches maturity detection using genetics algorithms," *Smart Agricultural Technology*, vol. 6, p. 100364, Dec. 2023, doi: 10.1016/j.atech.2023.100364.

[5] S. N. Shaharuzzaman, F. H. Hashim, M. S. Sajab, and A. B. Huddin, "Analysis of Free Fatty Acids (FFA) in Palm Oils Based on the Raman Spectra," in *2023 IEEE International Conference on Automatic Control and Intelligent Systems (I2CACIS)*, 2023, pp. 132–137. doi:10.1109/I2CACIS57635.2023.10193495.

[6] A. Ruswanto, A. H. Ramelan, D. Praseptiangga, and I. B. B. Partha, "Effects of ripening level and processing delay on the characteristics of oil palm fruit bunches," *Int J Adv Sci Eng Inf Technol*, vol. 10, no. 1, pp. 389–394, 2020, doi: 10.18517/ijaseit.10.1.10987.

[7] R. Sinambela, T. Mandang, I. D. M. Subrata, and W. Hermawan, "Application of an inductive sensor system for identifying ripeness and forecasting harvest time of oil palm," *Sci Hortic*, vol. 265, p. 109231, Apr. 2020, doi: 10.1016/j.scienta.2020.109231.

[8] L. A. A. Antwi, F. Nimoh, P. Agyemang, and I. A. Apike, "Perception and adoption of free fatty acid reduction techniques by small scale palm oil processors: Evidence from Ghana," *J Agric Food Res*, vol. 11, p. 100462, Mar. 2023, doi: 10.1016/j.jafr.2022.100462.

[9] P. Ibba, A. Falco, B. D. Abera, G. Cantarella, L. Petti, and P. Lugli, "Bio-impedance and circuit parameters: An analysis for tracking fruit ripening," *Postharvest Biol Technol*, vol. 159, p. 110978, Jan. 2020, doi: 10.1016/j.postharvbio.2019.110978.

[10] J. Juansah, I. W. Budiastra, K. Dahlan, and K. B. Seminar, "Electrical Properties of Garut Citrus Fruits at Low Alternating Current Signal and its Correlation with Physicochemical Properties During Maturation," *Int J Food Prop*, vol. 17, no. 7, pp. 1498–1517, Aug. 2014, doi: 10.1080/10942912.2012.723233.

[11] L. Tang, S. Gao, W. Wang, X. Xiong, W. Han, and X. Li, "Moisture Content Detection of Tomato Leaves Based on Electrical Impedance Spectroscopy," *Commun Soil Sci Plant Anal*, pp. 1–15, Oct. 2023, doi:10.1080/00103624.2023.2274046.

[12] P. Bertemes-Filho, W. Laus Bertemes, R. Cavalieri, A. Torres Paré, J. Spessatto, and D. Savi, "Ripening classification of bananas (Musa acuminate) using electrical impedance spectroscopy and support vector machine," *Int J Biosens Bioelectron*, vol. 6, no. 4, pp. 99–101, 2020, doi: 10.15406/ijbsbe.2020.06.00195.

[13] S. Shekhar and K. Prasad, "Nondestructive Evaluation of Moisture Content for Spinach Leaf Powder Using Complex Impedance Spectroscopy," *Journal of the ASABE*, vol. 66(2), pp. 415–421, 2023, doi: 10.13031/ja.14873.

[14] G. M. Stojanović, Sinha A, Ali A, Jeoti V, Radoičić M, Marković D, Radetić M, "Impedance analysis of milk quality using functionalized polyamide textile-based sensor," *Comput Electron Agric*, vol. 191, p. 106545, Dec. 2021, doi: 10.1016/j.compag.2021.106545.

[15] S. Huh, H.-J. Kim, S. Lee, J. Cho, A. Jang, and J. Bae, "Utilization of Electrical Impedance Spectroscopy and Image Classification for Non-Invasive Early Assessment of Meat Freshness," *Sensors*, vol. 21, no. 3, p. 1001, Feb. 2021, doi: 10.3390/s21031001.

[16] W. Huang, J. Xia, X. Wang, Q. Zhao, M. Zhang, and X. Zhang, "Improvement of non-destructive detection of lamb freshness based on dual-parameter flexible temperature-impedance sensor," *Food Control*, vol. 153, p. 109963, Nov. 2023, doi:10.1016/j.foodcont.2023.109963.

[17] A. C. F. de O. Meira, L. C. de Morais, M. M. de O. Paula, S. M. Pinto, and J. V. de Resende, "Application of electrical impedance spectroscopy for the characterisation of yoghurts," *Int Dairy J*, vol. 141, p. 105625, Jun. 2023, doi: 10.1016/j.idairyj.2023.105625.

[18] S. Hao, J. Yuan, J. Cui, W. Yuan, H. Zhang, and H. Xuan, "The rapid detection of acacia honey adulteration by alternating current impedance spectroscopy combined with 1H NMR profile," *LWT*, vol. 161, p. 113377, May 2022, doi: 10.1016/j.lwt.2022.113377.

[19] N. F. Chin-Hashim, A. Y. Khaled, D. Jamaludin, and S. Abd Aziz, "Electrical Impedance Spectroscopy for Moisture and Oil Content Prediction in Oil Palm (Elaeis guineensis Jacq.) Fruitlets," *Plants*, vol. 11, no. 23, Dec. 2022, doi: 10.3390/plants11233373.

[20] W. Ji, C. Tang, B. Xu, and G. He, "Contact force modeling and variable damping impedance control of apple harvesting robot," *Comput Electron Agric*, vol. 198, Jul. 2022, doi:10.1016/j.compag.2022.107026.

[21] J. W. Lai, H. R. Ramli, L. I. Ismail, and W. Z. Wan Hasan, "Oil Palm Fresh Fruit Bunch Ripeness Detection Methods: A Systematic Review," *Agriculture*, vol. 13, no. 1, p. 156, Jan. 2023, doi:10.3390/agriculture13010156.

[22] M. Zhuang, G. Li, K. Ding, and G. Xu, "Research on the application of impedance control in flexible grasp of picking robot," *Advances in Mechanical Engineering*, vol. 15, no. 4, p. 168781322311610, Apr. 2023, doi: 10.1177/16878132231161016.

[23] J. Cheng, P. Yu, Y. Huang, G. Zhang, C. Lu, and X. Jiang, "Application Status and Prospect of Impedance Spectroscopy in Agricultural Product Quality Detection," *Agriculture*, vol. 12, no. 10, p. 1525, Sep. 2022, doi: 10.3390/agriculture12101525.

[24] P. Jash, R. K. Parashar, C. Fontanesi, and P. C. Mondal, "The Importance of Electrical Impedance Spectroscopy and Equivalent Circuit Analysis on Nanoscale Molecular Electronic Devices," *Adv Funct Mater*, vol. 32, no. 10, Mar. 2022, doi:10.1002/adfm.202109956.

[25] D. Wu, J. Sun, R. Silvennoinen, and T. Repo, "Root injury detection by impedance loss factor and hydraulic conductance of apple (Malus domestica), blackcurrant (Ribes nigrum) and blueberry (Vaccinium corymbosum) nursery plants," *Sci Hortic*, vol. 328, p. 112864, Mar. 2024, doi: 10.1016/j.scienta.2024.112864.

[26] T. Kojic, M. Simić, M. Vučinić-Vasić, and G. M. Stojanović, "Sensing system based on knitted electrodes for fruit quality evaluation," *J Food Eng*, vol. 353, p. 111544, Sep. 2023, doi:10.1016/j.jfoodeng.2023.111544.

[27] G. W. Jr. Latimer, "General Methods," in *Official Methods of Analysis of AOAC INTERNATIONAL*, R. L. Beine, Ed., Oxford University PressNew York, 2023. doi: 10.1093/9780197610145.003.029.

[28] Piekutowska M, Niedbała G, Piskier T, Lenartowicz T, Pilarski K, Wojciechowski T, Pilarska A, Czechowska-Kosacka A, "The Application of Multiple Linear Regression and Artificial Neural Network Models for Yield Prediction of Very Early Potato Cultivars before Harvest," *Agronomy*, vol. 11, no. 5, p. 885, Apr. 2021, doi:10.3390/agronomy11050885.

[29] B. Konakoglu and A. Akar, "Geoid undulation prediction using ANNs (RBFNN and GRNN), multiple linear regression (MLR), and interpolation methods: A comparative study," *Earth Sciences Research Journal*, vol. 25, no. 4, pp. 371–382, 2021, doi:10.15446/esrj.v25n4.91195.

[30] D. J. S. Chong, Y. J. Chan, S. K. Arumugasamy, S. K. Yazdi, and J. W. Lim, "Optimisation and performance evaluation of response surface methodology (RSM), artificial neural network (ANN) and adaptive neuro-fuzzy inference system (ANFIS) in the prediction of biogas production from palm oil mill effluent (POME)," *Energy*, vol. 266, p. 126449, Mar. 2023, doi: 10.1016/j.energy.2022.126449.

[31] S. Ramjan and J. Sunkpho, *Principles and Theories of Data Mining with RapidMiner*. in Advances in Computer and Electrical Engineering. IGI Global, 2023. doi: 10.4018/978-1-6684-4730-7.

[32] N. Baharun, N. F. M. Razi, S. Masrom, N. A. M. Yusri, and A. S. A. Rahman, "Auto Modelling for Machine Learning: A Comparison Implementation between Rapid Miner and Python," *International Journal of Emerging Technology and Advanced Engineering*, vol. 12, no. 5, pp. 15–27, May 2022, doi: 10.46338/ijetae0522_03.

[33] D. J. Murphy, B. O' Brien, M. O' Donovan, T. Condon, and M. D. Murphy, "A near infrared spectroscopy calibration for the prediction of fresh grass quality on Irish pastures," *Information Processing in Agriculture*, vol. 9, no. 2, pp. 243–253, Jun. 2022, doi:10.1016/j.inpa.2021.04.012.